Hindawi
International Journal of Polymer Science
Volume 2020, Article ID 9627954, 7 pages
https://doi.org/10.1155/2020/9627954

Research Article

Multicomponent Nanocomposites for Complex Anticancer Therapy: Effect of Aggregation Processes on Their Efficacy

Nataliya Kutsevol,[1] **Yuliia Kuziv**,[1] **Tetiana Bezugla**,[1] **Vasyl Chumachenko**,[1] **and Vasyl Chekhun**[2]

[1]*Taras Shevchenko National University of Kyiv, 60 Volodymyrska Str., 01602 Kyiv, Ukraine*
[2]*R.E. Kavetsky Institute of Experimental Pathology, Oncology and Radiobiology, 45 Vasylkivska Str., 03022 Kyiv, Ukraine*

Correspondence should be addressed to Yuliia Kuziv; garaguts.yulia.fox@gmail.com

Received 7 February 2020; Revised 14 April 2020; Accepted 20 April 2020; Published 5 May 2020

Guest Editor: Can Yang Zhang

Multicomponent nanocomposites for anticancer therapy were prepared, characterized, and tested for their antitumor efficacy. The water-soluble star-like dextran-graft-polyacrylamide copolymer was used as a nanoplatform for the creation of polymer-based multicomponent drug delivery systems for photodynamic and combined (photodynamic+chemotherapy) antitumor therapy. The three-component nanocomposites with incorporated gold nanoparticles and photosensitizer and the four-component ones additionally loaded by Doxorubicin into polymer nanoplatform were studied at 25 and 37°C by transmission electron microscopy and dynamic light scattering. Nanocomposites were tested for their photodynamic cytotoxicity for the cell line of breast cancer MCF-7/S. Three-component nanocomposites demonstrated higher efficacy than the four-component ones. The decrease in the activity of the four-component systems is explained by the aggregation process caused by the introduction of an additional component, which leads to a decrease in the hydrophilic-hydrophobic balance of the polymer macromolecule.

1. Introduction

Actual cancer statistics indicate the need for innovative approaches, including nanotechnology, for efficient cancer diagnosis and therapy. Currently, the malignant tumor treatments use radiation, overheating (hyperthermia), excess oxygen (hyperoxygenation), and some harmful chemical substances or mutagens [1]. To improve treatment methods, researchers combine various inhibitory effects on cancer cells. Sometimes, anticancer drugs use several ways to destroy tumors [2].

In photothermal therapy (PTT) and photodynamic therapy (PDT), the desired effects of heat generation by metal nanoparticles and activation of photosensitizers (PS) occur in response to applied irradiation with specific light wavelengths. Recent studies have shown a synergistic effect obtained by the simultaneous use of PTT and PDT [3, 4]. Cytotoxic photothermal heating together with reactive singlet oxygen can trigger apoptotic and necrotic cancer cell death [2, 5]. The combination of multifunctional plasmonic nanoparticles and fluorescent photodynamic agents activated by near-infrared lasers has been the subject of research with encouraging results [3–6].

Gold nanoparticles (AuNPs) are known to be a photothermal agent with good biocompatibility and chemical inactivity. Their surface plasmon resonance (SPR) effect is highly efficient in converting light to heat, which leads to hyperthermia [7]. The SPR peak of AuNPs can be adjusted to the near-infrared region by controlling the geometrical parameters of the particles, such as size and shape [8]. Hyperthermia-induced cytotoxicity occurs within 1 h at 42°C, which can be shortened using higher temperatures [9]. Also, AuNPs can be easily accumulated in the tumor tissue due to the increased permeability and retention effect of the tumor [10].

Being incorporated into the cancer cells, AuNPs increase the reactive oxygen species generated by the cells, thereby affecting cell function [11]. However, AuNPs are more commonly used as carriers of photosensitizers. The molecules of

most photosensitizers are hydrophobic, and they require delivery systems to accomplish their cancer therapeutic effects [12, 13]. To increase the accumulation of PS in the tumor, it is advisable to combine it with gold nanoparticles, which are tropical to the tumor tissue and can serve as carriers of PS molecules [10]. Some of the scientific groups have reported that gold nanoparticles enhance not only the accumulation of PS but also the development of reactive oxygen species [14]. They demonstrated that complex compound AuNPs/photosensitizer/phase transfer reagents achieved higher singlet oxygen species generation compared to free photosensitizers [15].

Modern advances in drug delivery are now predicated upon water-soluble polymers with special characteristics in a soluble state [7, 10]. These polymers can be promising carriers not only for cytotoxic molecules but also for different nanosized objects. There is evidence of using polymer carriers for metal nanoparticles and hydrophobic organic substances simultaneously [16]. Polymer nanosystems are generated to achieve controlled drug release and target the delivery of hydrophobic drugs [17, 18]. In some cases, the conjecturable harmful effects on cancer cells can be enhanced by using polymer-drug conjugates with mutually reinforcing components. As it was shown in *in vitro* experiments on malignant cell line MT-4, a nanocomposite consisting of AuNPs and photosensitizer Chlorin e6 in a dextran-graft-polyacrylamide matrix demonstrated a twofold increase of photodynamic efficiency compared to a free photosensitizer [19].

Nanotechnology allows creating novel multicomponent drug delivery systems consisting of several components, for example, metal nanoparticles, photosensitizer, and anticancer chemical agent incorporated into the polymer matrix. Here, we focused on the synthesis and study of nanocomposites containing AuNPs for PTT, Chlorin e6 for PDT, and Doxorubicin for chemotherapy loaded into a water-soluble polyacrylamide-based polymer. The main purpose of the study was to understand the process occurring during the formation of multicomponent nanosystems at physiological temperatures (25 and 37°C).

2. Materials and Methods

2.1. Polymer Nanocarrier and Nanosystem Syntheses

2.1.1. Reagents. Tetrachloroauric acid, sodium borohydride, and Hank's balanced salt solution were purchased from Sigma-Aldrich (USA). Dimethyl sulfoxide (DMSO) was obtained from Serva (Germany). All reagents were of analytical purity and were used without further purification.

Chlorin e6 (Ce6) (Santa Cruz Biotechnology, USA) and Doxorubicin hydrochloride (Dox) (Sigma-Aldrich, USA) were used without further purification.

Double distilled water was used when needed.

2.1.2. Polymer Nanocarrier. Copolymer dextran-graft-polyacrylamide (D-g-PAA) in anionic form was used as a polymer matrix for gold nanoparticle synthesis as well as for the fabrication of nanosystems loaded with AuNPs, photosensitizer Ce6, and Dox. Synthesis and peculiarities of the macromolecular structure of star-like copolymer D-g-PAA were discussed in detail in [20]. D-g-PAA has dextran core ($Mw = 70 \cdot 105$ g/mol) and five grafted PAA chains. The average molecular weight of D-g-PAA (Mw) is equal to $2.15 \cdot 10^6$ g/mol, a radius of gyration (Rg) 85 nm, and polydispersity (Mw/Mn) 1.75. The anionic form of this copolymer was obtained via alkaline hydrolysis: 2 g of D-g-PAA was dissolved in 200 ml of distilled water, and then, the required amount of NaOH solution was added to it. The mixture was kept in a water bath at 50°C. The probes were taken in 30 min and precipitated by acetone. All samples were freeze-dried.

Size-exclusion chromatography coupled with light scattering was used for polymer sample characterization. SEC analysis was carried out by using a multidetection device consisting of an LC-10AD Shimadzu pump (throughput $0.5\ \text{ml} \cdot \text{mn}^{-1}$), an automatic injector WISP 717+ from Waters, 3 coupled 30 cm-Shodex OH-pak columns (803HQ, 804HQ, and 806HQ), a multiangle light scattering detector DAWN F from Wyatt Technology, and a differential refractometer R410 from Waters. Distilled water containing 0.1 M $NaNO_3$ was used as eluent. The degree of conversion of nonionic samples to ionic form was analyzed using a potentiometric titration of hydrolyzed samples. The content of carboxylate groups for hydrolyzed copolymer was approximately 37% [20]. Hereinafter, the copolymer D-g-PAA in the anionic form will be designated as Polymer.

2.1.3. Synthesis of Nanosystem Polymer/AuNPs. AuNPs were synthesized by the chemical reduction of Au precursor (tetrachloroauric acid) in aqueous Polymer solution at 25°C. Firstly, 0.05 ml of tetrachloroauric acid solution (0.1 M) was added to 1 ml of Polymer solution (1 mg/ml) and stirred for 20 min. Then, 0.1 ml of aqueous $NaBH_4$ solution (0.1 M) was injected. The final solution turned ruby red thus indicating the formation of AuNPs. The Au sol is designated as Polymer/AuNPs throughout.

2.1.4. Synthesis of Nanosystem Polymer/AuNPs/Ce6. A photosensitizer Ce6 is a poor water-soluble substance [21], so a stock solution of Ce6 (0.182 mg/ml) was prepared in DMSO. Then, 0.55 ml of this solution was mixed with 0.27 ml of distilled water. Finally, this mixture was added to 1.15 ml of Polymer/AuNP nanosystem under constant stirring. Thus, a three-component nanosystem was obtained, and it is designated as Polymer/AuNPs/Ce6.

2.1.5. Synthesis of Nanosystem Polymer/AuNPs/Dox. To prepare a three-component nanosystem containing a chemotherapeutic drug, 0.27 ml of the Dox solution (0.147 mg/ml) was mixed with 0.55 ml of distilled water; then, this mixture was added to 1.15 ml of Au sol (Polymer/AuNPs) under constant stirring. This system is designated as Polymer/AuNPs/Dox.

2.1.6. Synthesis of Nanosystem Polymer/AuNPs/Ce6/Dox. Four-component nanosystem was prepared using the Au sol synthesized in the Polymer solution. 0.27 ml of Dox (0.147 mg/ml) and 0.55 ml of Ce6 (0.182 mg/ml) solutions

were added to 1.15 ml of Polymer/AuNP solution under constant stirring. This system is designated as Polymer/AuNPs/Ce6/Dox.

2.2. Methods

2.2.1. Transmission Electron Microscopy (TEM). The observations of the AuNPs were carried out employing two TEMs, Tecnai G2 (ssCCD Eagle Camera) and CM12 (FEI, Eindhoven Netherlands) (Megaview SIS Camera). Copper grids with a plain carbon film were used for sample preparation (Elmo, Cordouan Technologies, Bordeaux, France). A 5 μl drop was deposited and let adsorbed for 1 min, and then, the excess of the solution was removed with a piece of filter paper.

2.2.2. Dynamic Light Scattering (DLS). DLS measurements were carried out using Zetasizer Nano ZS90 (Malvern Instruments Ltd., UK). The apparatus contains a 4 mW He-Ne laser with a wavelength of 632.8 nm. The scattered light is detected at an angle of 173° (backscattering).

Three-component nanosystems Polymer/AuNPs/Ce6 and Polymer/AuNPs/Dox and four-component nanosystem Polymer/AuNPs/Ce6/Dox were studied by DLS at 25 and 37°C. At the indicated temperature, the samples are kept for 5 minutes to achieve equilibrium. At least 10 correlation curves for each temperature point were processed by the CONTIN algorithm [22]. This is known to be reliable for complex systems to obtain hydrodynamic diameter (HD) distributions [23].

For correct analysis of processes occurring in multicomponent nanosystems, the authors' program or data treatment was used [24].

2.2.3. Evaluation of Dark Cytotoxicity and Photocytotoxic Activity of Nanocomposites. The cell line of breast cancer MCF-7/S was used for the experiments. The samples were obtained from a cell bank of human and animal tissue lines of the R.E. Kavetsky Institute of Experimental Pathology, Oncology and Radiobiology of National Academy of Sciences of Ukraine. Suspension cultures were grown in vitro in a complete nutrient medium of RPMI 1640 (Sigma-Aldrich, USA) with 2% L-glutamine, 10% embryonic serum calf (ETC; Biowest, France), and 40 μg/ml gentamicin at 37°C and in a humid atmosphere with the content of 5% CO_2. For the evaluation of dark cytotoxicity of nanoparticles and nanocomposites, the calculation of live/dead cells was determined in the MTT test after their staining with trypan blue [25].

For the *in vitro* study of the photodynamic effect of nanocomposites, the cells were incubated with nanosystems of different compositions for 1.5 h at 37°C. The samples were washed three times from unbound PS and irradiated in a Hanks solution with laser light. After that, the cells were transferred to the culture medium and incubated for 18-20 h at 37°C for the development and completion of apoptosis or necrosis in them. Then, the cell viability was determined in the MTT test. Each experiment was repeated at least 5 times.

A semiconductor laser (PMNP Photonikik Plus, Cherkasy) with a wavelength of 660 nm, which coincides with one of the Ce6 absorption maxima, was used as a light source for photodynamic damage to cells.

3. Results and Discussion

It was reported [26, 27] that D-g-PAA copolymers in both nonionic and anionic forms are not cytotoxic, and they can be absorbed by murine macrophages. These polymers were used as a base for the creation of the hybrid composites containing gold nanoparticles. The systems obtained were examined against breast cancer MCF-7 cell line and MT-4 (human T-cell leukemia) cell line [28]. The results proved low *in vitro* toxicity of examined composite like Polymer/AuNP sample even in high doses.

Our recent studies have shown higher photodynamic *in vivo* and *in vitro* efficiency against MT-4 cells (human T-cell leukemia) of a nanocomposite containing AuNPs and photosensitizer Ce6 incorporated into the star-like copolymer D-g-PAA in the anionic form in comparison with the same nanocomposite based on the nonionic polymer counterpart [26]. Also, the D-g-PAA copolymer in anionic form has demonstrated high efficiency as a nanocarrier for anticancer drugs Cisplatin and Doxorubicin when tested against K-562 (human chronic myelogenous leukemia cell line), U-937 (human histiocytic lymphoma cell line), and HeLa cells (cervical cancer) [27, 29]. Thus, the idea was to create nanocomposite for complex photothermal, photodynamic, and chemotherapy, namely, to synthesize Polymer-based nanocomposite loaded with AuNPs, photosensitizer Chlorin e6, and anticancer drug Doxorubicin hydrochloride simultaneously.

For the synthesis of the D-g-PAA copolymers, the cerium-ion-induced redox initiation method was used [20]. The average number of grafts per dextran molecule (n) is dependent on the ratio of Ce(IV) ions to dextran molecules [20]; this value was equal to 5. The mechanism of Ce(IV) initiation is based on the formation of the chelate complex, which while decomposing generates free radical sites on the polysaccharide backbone. These active free radicals trigger PAA chain growth in the presence of an acrylic monomer. The reaction path is shown below:

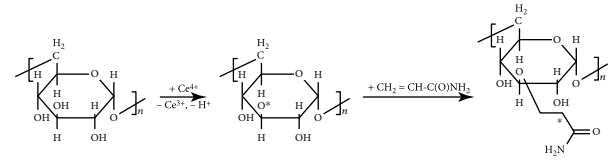

The peculiarities of the molecular structure of branched copolymers dextran-graft-polyacrylamide in nonionic and ionic forms were discussed in [20]. These copolymers are star-like, consisting of the dextran core and long polyacrylamide grafts. The average conformation of grafted PAA chains depends on the grafting ratio. For the D-g-PAA copolymer used in the present work, the PAA grafts have worm-like conformation. The ionic form of this copolymer was obtained after saponification. The branched polyelectrolyte has an extremely expanded conformation of the grafted chains in solution [20]. Alkaline hydrolysis of D-g-PAA

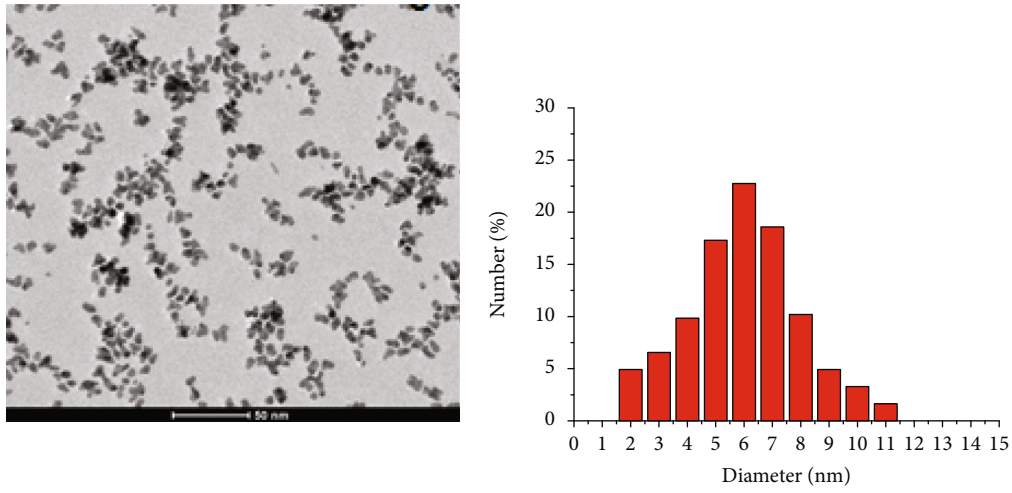

Figure 1: TEM image of AuNPs in Polymer/AuNP nanosystem (a) and size distribution histogram of AuNPs in this sample (b).

copolymers was not accompanied by irrelevant processes (the breaking or cross-linking of macromolecules) as was confirmed by SEC analysis of source and saponified samples. The branched polymers have a higher local concentration of functional groups in comparison with their linear analogs. These structural peculiarities are advantageous for biomedical applications [20].

AuNPs were synthesized *in situ* in a water solution of D-g-PAA in the anionic form. According to the TEM data, the Polymer/AuNP system contains gold particles of 2-11 nm in size with not completely spherical shape (Figure 1(a)). The size distribution of AuNPs is shown in Figure 1(b).

DLS analysis of heterogeneous Polymer/AuNP solution revealed several scattering objects that can be divided into two groups with well-defined maxima. According to the molecular parameter of the polymer matrix represented above, the peak with a maximum at 70 nm (Figure 2) corresponds to the macromolecules of D-g-PAA in anionic form loaded with AuNPs. The weakly pronounced peaks in the region of 2-11 nm on the weighted intensity distribution can be attributed to AuNPs. The scattering intensity of small metal nanoparticles about 10 nm in size is drastically lower in comparison with large polymer coils [30]. That is why the intensity distribution for small nanoparticles does not allow evaluating the average size and polydispersity of AuNPs in nanosystems by using DLS.

Three-component Polymer/AuNPs/Ce6 and Polymer/-AuNPs/Dox and four-component Polymer/AuNPs/Ce6/Dox nanosystems were prepared by the method described above, then were centrifuged. The absorption spectra of the supernatant showed the absence of Ce6 and Dox in solution, thus indicating its total incorporation into polymer nanocarrier. These nanocomposites were used for DLS and *in vitro* anticancer examination.

The size distributions of scattering nanoobjects in the three-component Polymer/AuNPs/Ce6 nanosystem at different temperatures are shown in Figures 3(a) and 3(b). DLS data demonstrate several types of scattering nanoobjects

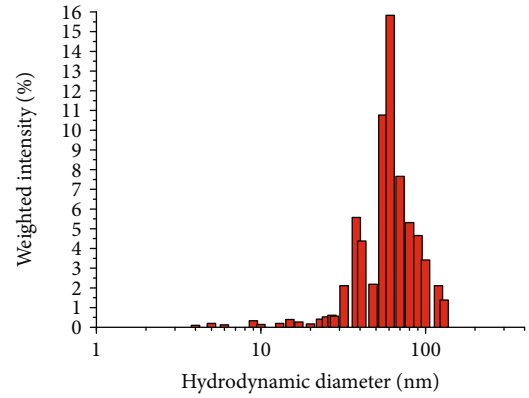

Figure 2: Hydrodynamic diameter distributions of scattering objects in Polymer/AuNP nanosystem.

in this system at 25°C (Figure 3(a), black curve). The first maximum corresponds to AuNPs of about 10 nm in size. The second maximum can be attributed to the individual AuNP-loaded macromolecules with coil diameter near 70-80 nm. The third maximum deals with the presence of aggregates of macromolecules with AuNPs inside. The size of these nanoobjects is equal to 200-500 nm. Changes in dimensional characteristics of this nanosystem occur at 37°C. Two distinct peaks are registered in the size range above 100 nm thus indicating the reorganization of aggregates (Figure 3(b), black curve). In contrast to other nanosystems, the fraction of aggregates with the less sizes (100-200 nm) in Polymer/-AuNPs/Ce6 system is significant. That may be caused by the partial destruction of hydrogen bonds between grafts of polymer nanocarrier at 37°C. However, the size of the gold nanoparticles and the size of nanoobjects corresponding to individual macromolecules with incorporated AuNPs do not change.

According to DLS data obtained from an experiment with Polymer/AuNPs/Dox nanosystem at 25°C, this sample contains AuNPs of 10 nm in size, individual Polymer

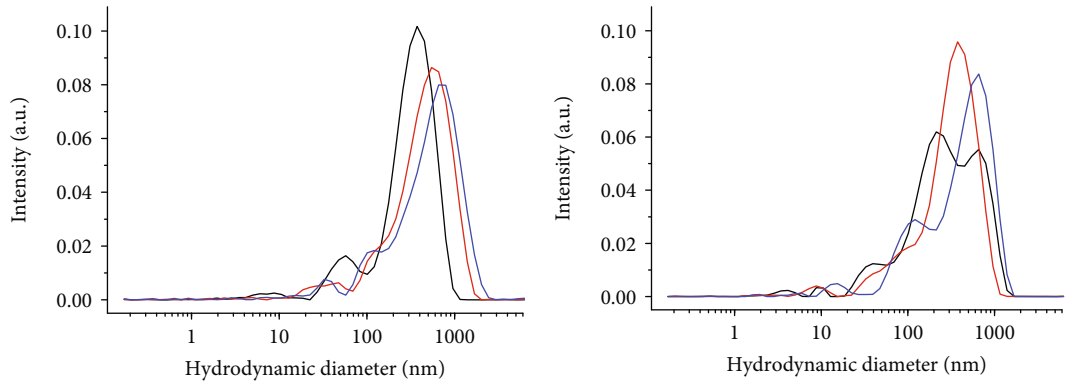

Figure 3: The dependence of the normalized scattering intensity on the hydrodynamic diameter of the scattering objects for the Polymer/AuNPs/Ce6 (black), Polymer/AuNPs/Dox (red), and Polymer/AuNPs/Ce6/Dox (blue) nanosystems at 25°C (a) and 37°C (b).

Table 1: Composition of nanocomposites used for in vitro tests on MCF-7/S breast cancer cells.

Sample	$C_{Polymer}$ (mkg/ml)	C_{AuNPs} (mkg/ml)	C_{Ce6} (mkg/ml)	C_{Dox} (mkg/ml)
Nanocomposite 1	508	500	50	—
Nanocomposite 2	508	500	50	20
Nanocomposite 3	508	500	50	20 (extempore)

macrocoils with incorporated AuNPs (60-70 nm), and its macromolecular aggregates (approximately 100-110 nm and 500 nm) (Figure 3(a), red curve). Compared to Polymer/-AuNPs/Ce6 nanosystem, the aggregation process in Polymer/AuNPs/Dox nanosystem is more significant. With an increase in temperature to 37°C, changes in the dimensional characteristics of nanosystems are registered, namely, the reduction in the size of the greatest aggregates occurs (Figure 3(b), red curve). These changes could be caused by two processes—the destruction of some aggregates or the compression of macromolecular coils. However, the latter process seems unlikely because no additional component that could bind to the functional groups of the polymer was added. The size of the AuNPs and the size of the nanoobjects, which consist of individual macromolecules with incorporated AuNPs, do not change.

For Polymer/AuNPs/Ce6/Dox nanosystem, there are several scattering objects on the DLS curve at 25°C (Figure 3(a), blue curve). AuNPs of 10 nm in size, individual macromolecules with incorporated AuNPs (about 60-70 nm), and its aggregates (100-200 nm and about 800 nm) can be observed. The increased ability to aggregate in this nanosystem compared to those described above seems to be the result of an increase in the number of components included in the Polymer macrocoils. That leads to a change in the hydrophobic-hydrophilic balance of the Polymer molecules. Polymer loaded with considered components become more hydrophobic since hydrophilic acrylamide and carboxylate groups are blocked both by Ce6 and Dox molecules.

There are no significant changes in sizes of scattering objects for Polymer/AuNPs/Ce6/Dox nanosystem at 37°C. Only some decreases of the hydrodynamic radius of the greatest aggregates are observed (Figure 3(b), blue curve). It can be caused by reorganization in the nanosystems due to the partial destruction of internal and external hydrogen bonds between grafts of polymer nanocarrier. The size of AuNPs and the size of the nanoobjects consisting of individual macromolecules with AuNPs do not change. However, an increase in aggregation ability in a four-component nanosystem in comparison with three-component ones at studied temperatures is evident. As a whole, four-component nanosystem Polymer/AuNPs/Ce6/-Dox contains macromolecular aggregates that are greater in size compared to those in both Polymer/AuNPs/Ce6 and Polymer/AuNPs/Dox nanosystems.

Polymer/AuNP/Ce6 and Polymer/AuNPs/Ce6/Dox nanosystems were tested for its PDT and dark cytotoxicity on MCF-7/S breast cancer cells. The compositions of tested nanosystems are shown in Table 1. Nanocomposite 1 and Nanocomposite 2 were presynthesized and kept in the refrigerator. Nanocomposite 3 was prepared by "extempore" way through the addition of Dox to the Polymer/AuNPs/Ce6 composition in 10 minutes before its mixing with the culture cells. As was shown, the individual Polymer and Polymer loaded with AuNPs have no significant cytotoxic effects on the cancer cells at the studied concentrations.

In the "control" experiment, the cancer cells were subjected to the same manipulations but without the addition of nanocomposites. It was shown that MCF-7/S cells were not sensitive to Nanocomposites 1 and 2 without external irradiation (Figure 4, blue bars). The "dark" measures demonstrated the same results on the survival of cells being incubated with the addition of the studied nanocomposites and in the "control" experiment.

However, a significant increase in the toxic properties of Nanocomposite 1 was registered after PDT (Figure 4, red

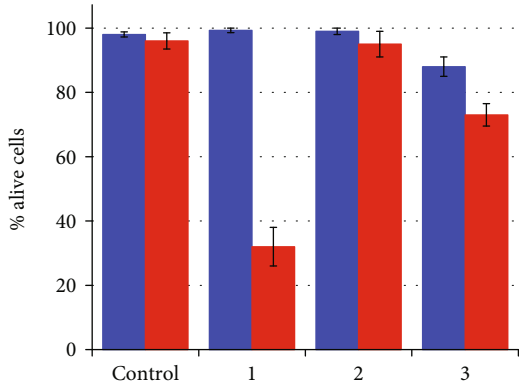

Figure 4: The survival of MCF-7/S cells after treatment with Nanocomposite 1 (1); Nanocomposite 2 (2); and Nanocomposite 3 (3) and in control experiment (control). Blue: "dark" measures; red: after PDT.

bars). Nanocomposite 2 contains the same amount of Ce6 as Nanocomposite 1, but the survival of cells after external irradiation is much higher for Nanocomposite 2 compared to Nanocomposite 1. The significant decrease in the efficiency of the four-component Nanocomposite 2 compared to the three-component Nanocomposite 1 may be a result of an increased aggregation of macromolecular coils containing the active ingredients of the system. Nanocomposite 3, prepared "ex tempore," demonstrated higher efficacy in comparison with Nanocomposite 2, despite the same content of ingredients. It may be due to the fact that the molecules of Dox-added extempore are not completely incorporated into polymer in 10 min. The system does not achieve equilibrium. Therefore, free Dox can be present in Nanosystem 3 that explains some "dark" toxicity effect for tumor cells as well as higher results on the cell death in the PDT experiment (Figure 4, blue bars).

Similar effects of decreasing efficiency of polymer nanosystems loaded with active components towards damage of cancer cells were revealed when the number of these components increased [31]. As it was reported in [27], the water-soluble polymer nanocarriers such as dextran-graft-(polyacrylamide-co-polyacrylic acid) loaded with chemotherapeutic substance Cisplatin demonstrated high toxicity to cancer cells. However, when the copolymers were conjugated with both AgNPs and Cisplatin, the three-component nanosystem showed a lower cytotoxic effect [27], which was caused by the aggregation process in multicomponent systems.

4. Conclusion

It is shown in the current work that the polymer-based multicomponent nanosystem Polymer/AuNPs/Ce6 demonstrated high efficacy in PDT, but the addition of the fourth component Dox to this composite resulted in a decrease of antitumor efficacy. The aggregation processes and formation of great aggregates in the four-component system Polymer/-AuNPs/Ce6/Dox seem to cause a decrease in the therapeutic effect in PDT.

The development of nanosystems for photodynamic therapy is in the focus of current biomedical research. It is possible to improve the effectiveness of cancer treatment due to the achievements of nanotechnology that provide an opportunity to develop complex therapeutic composites, but the use of multicomponent nanosystems needs a deep understanding of the processes occurring at its preparation to avoid some aggregation.

Data Availability

The data used to support the findings of this study are included within the article.

Conflicts of Interest

The authors declare that there is no conflict of interest regarding the publication of this paper.

References

[1] D. Feldman, "Polymers and polymer nanocomposites for cancer therapy," *Applied Science*, vol. 9, no. 18, p. 3899, 2019.

[2] R. Mendes, P. Pedrosa, J. C. Lima, A. R. Fernandes, and P. V. Baptista, "Photothermal enhancement of chemotherapy in breast cancer by visible irradiation of gold nanoparticles," *Scientific Reports*, vol. 7, no. 1, p. 10872, 2017.

[3] F. Ghorbani, N. Attaran-Kakhki, and A. Sazgarnia, "The synergistic effect of photodynamic therapy and photothermal therapy in the presence of gold-gold sulfide nanoshells conjugated indocyanine green on HeLa cells," *Photodiagnosis and Photodynamic Therapy*, vol. 17, pp. 48–55, 2017.

[4] B. Jang, J.-Y. Park, C.-H. Tung, I.-H. Kim, and Y. Choi, "Gold nanorod-photosensitizer complex for near-infrared fluorescence imaging and photodynamic/photothermal therapy *in vivo*," *ACS Nano*, vol. 5, no. 2, pp. 1086–1094, 2011.

[5] H. Kim and D. Lee, "Near-infrared-responsive cancer photothermal and photodynamic therapy using gold nanoparticles," *Polymers*, vol. 10, no. 9, p. 961, 2018.

[6] S. Veeranarayanan, M. S. Mohamed, A. C. Poulose et al., "Photodynamic therapy at ultra-low NIR laser power and X-ray imaging using Cu_3BiS_3 nanocrystals," *Theranostics*, vol. 8, no. 19, pp. 5231–5245, 2018.

[7] P. Kaur, M. L. Aliru, A. S. Chadha, A. Asea, and S. Krishnan, "Hyperthermia using nanoparticles–promises and pitfalls," *International Journal of Hyperthermia*, vol. 32, no. 1, pp. 76–88, 2016.

[8] C. L. Nehl and J. H. Hafner, "Shape-dependent plasmon resonances of gold nanoparticles," *Journal of Materials Chemistry*, vol. 18, no. 21, pp. 2415–2419, 2008.

[9] S. H. Beachy and E. A. Repasky, "Toward establishment of temperature thresholds for immunological impact of heat exposure in humans," *International Journal of Hyperthermia*, vol. 27, no. 4, pp. 344–352, 2011.

[10] L. A. Bennie, H. O. McCarthy, and J. A. Coulter, "Enhanced nanoparticle delivery exploiting tumour-responsive formulations," *Cancer Nano*, vol. 9, no. 1, p. 10, 2018.

[11] J. Peng and X. Liang, "Progress in research on gold nanoparticles in cancer management," *Medicine*, vol. 98, no. 18, p. e15311, 2019.

[12] Y. N. Konan, R. Gurny, and E. Allémann, "State of the art in the delivery of photosensitizers for photodynamic therapy,"

Journal of Photochemistry and Photobiology B: Biology, vol. 66, no. 2, pp. 89–106, 2002.

[13] C. Yao, L. Zhang, J. Wang et al., "Gold nanoparticle mediated phototherapy for cancer," *Journal of Nanomaterials*, vol. 2016, Article ID 5497136, 29 pages, 2016.

[14] E. Paszko, C. Ehrhardt, M. O. Senge, D. P. Kelleher, and J. V. Reynolds, "Nanodrug applications in photodynamic therapy," *Photodiagnosis and Photodynamic Therapy*, vol. 8, no. 1, pp. 14–29, 2011.

[15] S. J. Chadwick, D. Salah, P. M. Livesey, M. Brust, and M. Volk, "Singlet oxygen generation by laser irradiation of gold nanoparticles," *The Journal of Physical Chemistry C*, vol. 120, no. 19, pp. 10647–10657, 2016.

[16] W. B. Liechty, D. R. Kryscio, B. V. Slaughter, and N. A. Peppas, "Polymers for drug delivery systems," *Annual Review of Chemical and Biomolecular Engineering*, vol. 1, no. 1, pp. 149–173, 2010.

[17] N. Jawahar and S. N. Meyyanathan, "Polymeric nanoparticles for drug delivery and targeting: a comprehensive review," *International Journal of Health & Allied Sciences*, vol. 1, no. 4, pp. 217–230, 2012.

[18] N. R. Jabir, S. Tabrez, G. M. Ashraf, S. Shakil, G. A. Damanhouri, and M. A. Kamal, "Nanotechnology-based approaches in anticancer research," *International Journal of Nanomedicine*, vol. 7, pp. 4391–4408, 2012.

[19] V. A. Chumachenko, I. O. Shton, E. D. Shishko, N. V. Kutsevol, A. I. Marinin, and N. F. Gamaleia, "Branched copolymers dextran-graft-polyacrylamide as nanocarriers for delivery of gold nanoparticles and photosensitizers to tumor cells," in *Nanophysics, Nanophotonics, Surface Studies, and Applications*, O. Fesenko and L. Yatsenko, Eds., vol. 183, pp. 379–390, Springer Proceedings in Physics, 2016.

[20] M. Bezugly, N. Kutsevol, M. Rawiso, and T. Bezugla, "Water-soluble branched copolymers dextran-polyacrylamide and their anionic derivates as matrices for metal nanoparticles in situ synthesis," *Chemik*, vol. 66, no. 8, pp. 865–867, 2012.

[21] V. P. Savitskiy, V. P. Zorin, and M. P. Potapnev, "Accumulation of chlorine e6 derivatives in cells with different level of expression and function activity of multidrug resistance protein P-gp 170," *Experimental oncology*, vol. 27, no. 1, pp. 47–51, 2005.

[22] S. Provencher, "CONTIN: a general purpose constrained regularization program for inverting noisy linear algebraic and integral equations," *Computer Physics Communications*, vol. 27, pp. 229–242, 1992.

[23] A. Scotti, W. Liu, J. S. Hyatt et al., "The CONTIN algorithm and its application to determine the size distribution of microgel suspensions," *The Journal of Chemical Physics*, vol. 142, no. 23, p. 234905, 2015.

[24] V. Chumachenko, N. Kutsevol, Y. Harahuts, M. Rawiso, A. Marinin, and L. Bulavin, "Star-like dextran-graft-PNiPAM copolymers. Effect of internal molecular structure on the phase transition," *Journal of Molecular Liquids*, vol. 235, pp. 77–82, 2017.

[25] A. K. Kwok, C. K. Yeung, T. Y. Lai, K. P. Chan, and C. P. Pang, "Effects of trypan blue on cell viability and gene expression in human retinal pigment epithelial cells," *The British Journal of Ophthalmology*, vol. 88, no. 12, pp. 1590–1594, 2004.

[26] N. Kutsevol, A. Naumenko, Y. Harahuts et al., "New hybrid composites for photodynamic therapy: synthesis, characterization and biological study," *Applied Nanoscience*, vol. 9, no. 5, pp. 881–888, 2019.

[27] G. Telegeev, N. Kutsevol, V. Chumachenko et al., "Dextran-polyacrylamide as matrices for creation of anticancer nanocomposite," *International Journal of Polymer Science*, vol. 2017, Article ID 4929857, 9 pages, 2017.

[28] N. Kutsevol, Y. Harahuts, I. Shton et al., "In vitro study of toxicity of hybrid gold-polymer composites," *Molecular Crystals and Liquid Crystals*, vol. 671, no. 1, pp. 1–8, 2018.

[29] A. Yurchenko, N. Nikitina, V. Sokolova et al., "A novel branched copolymer-containing anticancer drug for targeted therapy:*in vitro* research," *Bionanoscience*, vol. 10, pp. 249–259, 2019.

[30] J. Stetefeld, S. A. McKenna, and T. R. Patel, "Dynamic light scattering: a practical guide and applications in biomedical sciences," *Biophysical Reviews*, vol. 8, no. 4, pp. 409–427, 2016.

[31] N. Kutsevol, A. Naumenko, V. Chumachenko, O. Yeshchenko, Y. Harahuts, and V. Pavlenko, "Aggregation processes in hybrid nanosystem polymer/nanosilver/cisplatin," *Ukrainian Journal of Physics*, vol. 63, no. 6, pp. 513–520, 2018.